Aqueous Dispersion of Conjugated Polymers by Colloidal Clays and Their Film Photoluminescence

Yi-Fen Lan,[†] Rong-Ho Lee,[‡] and Jiang-Jen Lin*[,†,§]

Institute of Polymer Science and Engineering, National Taiwan University, Taipei, 10617 Taiwan, Department of Chemical and Materials Engineering, National Yunlin University of Science and Technology, Douliou, Yunlin, 64002 Taiwan, and Department of Materials Science and Engineering, and Center of Nanoscience and Nanotechnology, National Chung Hsing University, Taichung, 402 Taiwan

Received: November 23, 2009; Revised Manuscript Received: December 19, 2009

The plate-shaped clays enabled us to disperse water-insoluble conjugated polymers (CPs) into a colloidal form and an aqueous process for making CP films. Simple pulverization of poly[2-methoxy-5-(2′-ethylhexyloxy)-1,4-phenylenevinylene] (MEH-PPV) with silicate clays rendered the powder mixture an unusual dispersing behavior in water. The most effective clay was selected from screening several natural and synthetic clays including synthetic fluorinated mica (Mica), sodium montmorillonite (MMT), synthetic smectite (SWN), and cationic layered double hydroxide (LDH). A high aspect ratio and intensive charge density (2.1 e nm^{-1}) of Mica were highly effective for promoting the CP dispersion. The enhancement for dispersing MEH-PPV is rated in the following trend: Mica > MMT > SWN > LDH. The result is rationalized by the influences of their geometric shape and ionic charge of clay on MEH-PPV in water. Two other representative CPs, sulfonated polyaniline (SPA) and triphenyl phosphine oxide cored polyaniline (TPOPA), were used to generalize the CP/clay colloidal behavior. All of the three CPs as in an aqueous form can be coated into hybrid films. Under an ultraviolet lamp, these films showed color emissions, orange for MEH-PPV/Mica, olive for SPA/Mica, and green for TPOPA/Mica, which are consistent with the photoluminescence measurements.

1. Introduction

Conjugated polymers (CPs) with various chemical structures, such as poly(*p*-phenylene),[1−3] poly(*p*-phenylene-vinylene),[4] poly(*p*-phenylene-ethynylene),[5] polyaniline,[6,7] poly(triacetylene),[8] poly(acetylene),[9] polythiophene,[10] polycarbazole,[11] and poly(fluorene),[12,13] are well documented for their properties and applications of electronic conductivity[14−16] and light-emitting devices.[17,18] Among the diversified applications, the process of fabricating devices may be limited by the inherent physical properties such as insolubility of the rigid-rod CPs.

Structural modification by attaching alkoxy or flexible alkyls to the main polymer backbone is the common approach for synthesizing soluble CPs.[1−13] With the enhancement of their solubility in organic mediums, the process may be improved for some applications in optoelectronics, microelectronics,[19,20] and their devices for sensors.[21,22] However, the structural modifications could be complicated procedures and have great influence on optical performance, and the modified CPs only can be dispersed in hazard-organic solvents, such as chloroform, dichloroform, and dichlorobenzene, etc. In a recent literature surveillance, syntheses of water-soluble CPs are found for the applications as fluorescence biosensors.[23,24] The synthesis generally involves the grafting anionic polar functionalities such as sulfonic, carboxylic, and phosphoric groups on the alkoxy side chain of the polymers.[25−30] One of the advantages for using water-borne CPs is to reduce the use of volatile organic solvents in fabricating devices. This "green process" can be important for advancing these nanomaterial applications. However, the complicated procedures for water-borne CP synthesis could be time consuming.

In our previous studies, the dispersion of nanomaterials could be controlled or enhanced by a unique mechanism of geometric shaped inhomogenesity (GSI). The pulverization of two nanomaterials with a large difference in geometric shaped will alternate their dispersed behavior by each other. The dispersion of carbon black,[31] silver nanoparticle,[32] and carbon nanotube[33] can be improved based on GSI. In this article, we report the uses of colloidal clays to aqueous dispersion of hydrophobic CPs based on GSI. Three representative CPs, poly[2-methoxy-5-(2′-ethylhexyloxy)-1,4-phenylenevinylene] (MEH-PPV), sulfonated polyaniline (SPA), and triphenyl phosphine oxide cored polyaniline (TPOPA), were allowed to mix and grind with the ionic clays of plate-like geometric shape. Among the screened clays, the synthetic fluorinated mica (Mica) was the most effective for dispersing CPs in water. The clays with high aspect-ratio geometric shape and ionic charges could well interact with the hydrophobic polymers through noncovalent bonding forces. By varying the clay species, the geometric shape was found to be one of the important factors for influencing the CP dispersion. The clay affecting CP dispersion is generalized by using representative CPs of polyaniline structures with rigid shape and making them into hybrid films. Their dispersion behavior and photophysical properties were characterized by ultraviolet−visible (UV−vis), photoluminescence (PL) spectrophotometry, and transmission electron microscopy (TEM).

2. Experimental Section

2.1. Materials. The conjugated polymer, poly[2-methoxy-5-(2′-ethylhexyloxy)-1,4-phenylenevinylene] (MEH-PPV), with a weight-average molecular weight (M_w) of 51 000 was purchased from Aldrich Chemical Co. Two other conjugated

* Corresponding author. E-mail: jianglin@ntu.edu.tw. Fax: +886-2-8369-1384. Tel.: +886-2-3366-5312.
[†] National Taiwan University.
[‡] National Yunlin University of Science and Technology.
[§] National Chung Hsing University.

10.1021/jp911117m
Published on Web 01/07/2010

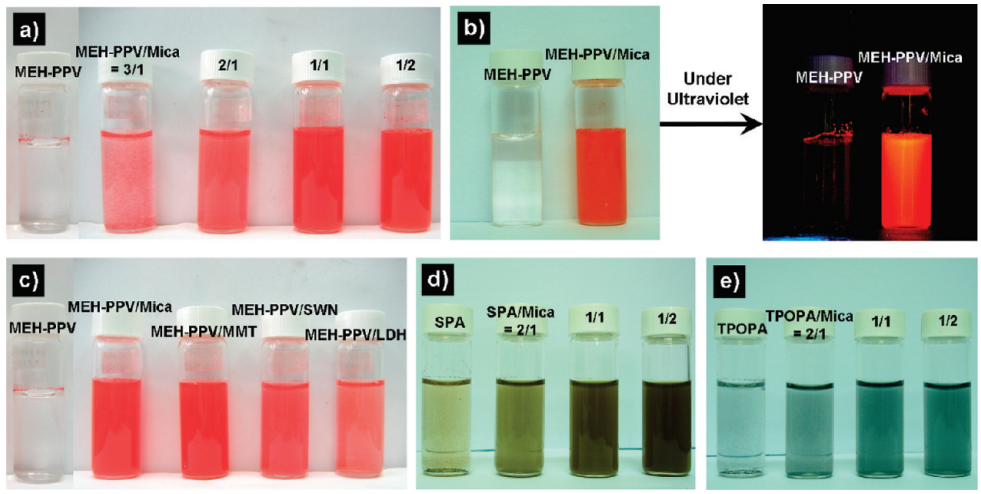

Figure 1. Dispersion of CP/Clay in water (1 mg CPs in 5 g of water): (a) MEH-PPV/Mica at 3/1, 2/1, 1/1, and 1/2 weight ratios, (b) MEH-PPV/Mica (1/1) under UV light, (c) MEH-PPV/Clay (1/1), Clay = Mica, MMT, SWN, and LDH, (d) SPA/Mica at 2/1, 1/1, and 1/2 ratios, and (e) TPOPA/Mica at 2/1, 1/1 and 1/2 ratios.

polymers, sulfonated polyaniline (SPA) and triphenyl phosphine oxide cored polyaniline (TPOPA), were prepared as previously described.[7,34] Both SPA and TPOPA are rigid structures with tubular and polygonal shape (see Supporting Information, Figure S1) and sluggishly dispersible in water. The chemical structures of MEH-PPV, SPA, and TPOPA are described in the Supporting Information, Figures S2, S3, and S4. Different species of clays, synthetic fluorinated mica (Mica, trade name as SOMASIF ME-100), and synthetic smectite (SWN, trade name as Lucentite SWN) were obtained from CO-OP Chemical Co. (Japan). Sodium montmorillonite (Na^+-MMT), supplied from Nanocor Co., is a Na^+ form of smectite clay with a cationic exchange capacity (CEC) of 1.2 mequiv g^{-1}. These anionic clays are irregular aggregates from their primary units consisting of silicate plates in stacks.[35] The platelike units are polygonal and polydisperse in geometric shape, carrying ionic charges and counterions ($\equiv SiO^-Na^+$) within the interlayer structure. The average plate dimension is 300 × 300 × 1 nm^3 for Mica, 100 × 100 × 1 nm^3 for MMT, and 80 × 80 × 1 nm^3 for SWN. The negative surface charge densities of Mica, MMT, and SWN are 2.1, 0.708, and 30 (e nm^{-2}), respectively.[36−38] Due to the presence of an intensive ionic charge character, these clays are capable of swelling and gelling in water.[39] With a similar platelike structure (ca. 200 × 200 × 1 nm^3) but with oppositely charged character, the layered double hydroxide (LDH) $[Mg_6Al_2(OH)_{16}]CO_3 \cdot 4H_2O$ was prepared according to the reported procedures.[40] The cationic LDH clay has the counterions of carbonates[41,42] and has a positive charge density of 1.5 (e nm^{-2}).[43]

2.2. Preparation of the MEH-PPV/Mica Hybrid. The preparation of the MEH-PPV/Mica hybrid is described below. The mixtures of MEH-PPV (1 mg) and Mica (1 mg) were ground thoroughly in an agate mortar and pestle. The sides of the mortar were occasionally scraped down with the pestle during grinding to ensure a thorough mixing. The powder mixture was washed from mortar and pestle using deionized water to have a solid content of 1 mg of MEH-PPV in 5 g of water. The MEH-PPV/Mica hybrids were prepared at a weight ratio of MEH-PPV/Mica = 3/1, 2/1, 1/1, and 1/2. During the mixing, ultrasonic vibration was applied for 2 min operated on BRANSON 5510R-DTH (135 W, 42 kHz).

2.3. Characterization. The aqueous dispersions of the CP/clay hybrid were analyzed by an ultraviolet−visible spectrophotometer (Perkin-Elmer Lambda 20 UV−vis spectrophotometer) and transmission electron microscopy (TEM; JEOL JEM-1230 TEM with Gatan Dual Vision CCD Camera and operated at 100 kV). The TEM samples were prepared by dropping the dispersion of 0.01% (w/w) CP/clay onto a carbon-coated copper grid and drying at room temperature. The CP hybrid films were prepared by dropping 0.1% (w/w) CP/clay solutions on a 10 × 10 mm glass substrate and drying at 80 °C. Both solutions and

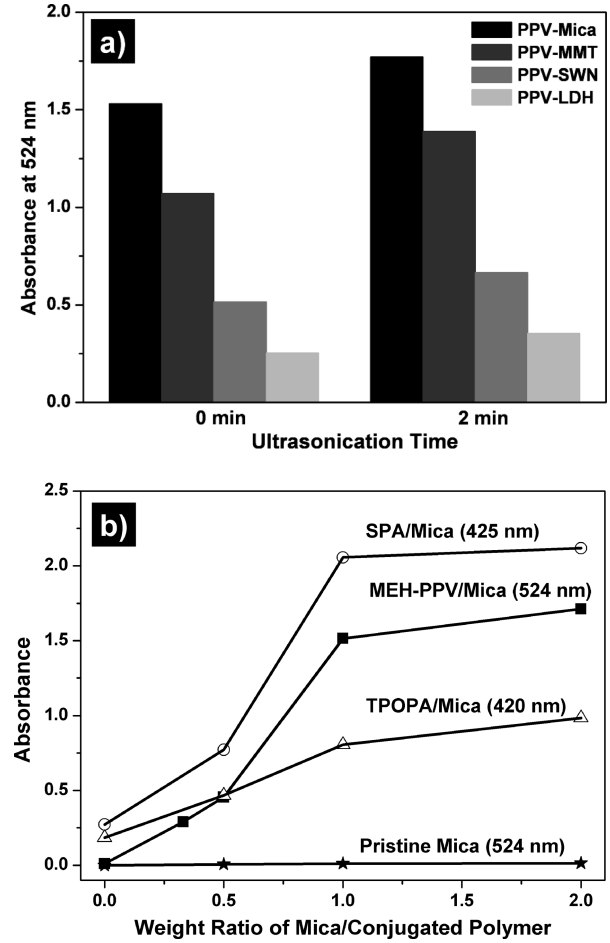

Figure 2. UV−vis absorbance of CP/clay in water: (a) MEH-PPV dispersed by Mica, MMT, SWN, or LDH, at weight ratio of 1/1 and (b) MEH-PPV, SPA, and TPOPA polymers dispersed by Mica at different weight ratios.

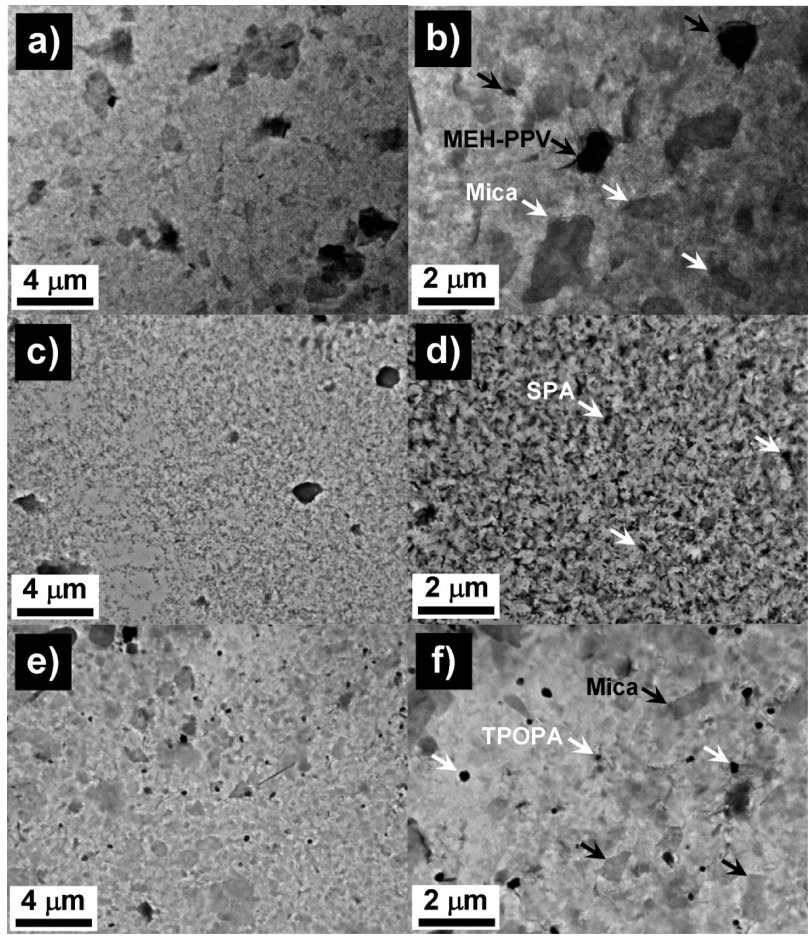

Figure 3. TEM images of CP/Mica dispersion (at 1/1 weight ratio) in water: MEH-PPV (a,b), SPA (c,d), and TPOPA (e,f).

films of the CP/clay hybrid were analyzed by a photoluminescence spectrophotometer LS45/55. The light-emitting phenomenon was observed under the UV light from a hand-held ultraviolet (UV) lamp, UVGL-85 (365 nm, 6 W, 115 V, 60 Hz, 0.12 A). A ZetaPlus zetameter (Brookhaven Instrument Corp., NJ) was used for characterizing the ionic property of the pristine clays and MEH-PPV/clay hybrids. Samples of aqueous suspension at 0.01 and 0.02 wt % were measured. The suspension pH was adjusted to pH 7 by either adding 0.5 M NaOH or HCl. The zeta potential was measured in the solution with an ionic strength of 0.2. The same instrument was used to estimate the average particle size of the clay particles.

3. Results and Discussion

3.1. Dispersion of CP/Clay in Water. Conjugated polymers are generally water-insoluble and require a substantial side-chain modification to improve their solubility for processing. Moreover, the layered silicate clays are well established for their swelling and colloidal properties.[39] With pulverizing together, both materials in powder form of the physical mixture altered their inherent aggregating behaviors and mutually affected their solvating abilities. To understand their dispersing behaviors, the representative MEH-PPV was selected for the initial tests. The clays including the fluorinated mica (Mica), sodium montmorillonite (MMT), synthetic clay (SWN), and a cationic type of layered double hydroxide (LDH) were screened. Four clays represent different anionic and cationic species with a range of average geometric size: Mica ($300 \times 300 \times 1$ nm^3), MMT ($100 \times 100 \times 1$ nm^3), SWN ($80 \times 80 \times 1$ nm^3), and LDH ($200 \times 200 \times 1$ nm^3). Due to the presence of intensive ionic charges, these clays are capable of swelling and gelling in water.[39] After physical pulverization, the MEH-PPV/Mica mixture showed an improvement in solvating ability in water, while the pristine MEH-PPV is only sluggishly dispersible. In Figure 1a, it is demonstrated that the MEH-PPV/Mica hybrid at 1/1 and 1/2 weight ratios is dispersible compared to a serious aggregation of MEH-PPV without Mica. The degree of dispersion can be differentiated by the naked eye from a red-color solution to an apparent solid aggregate. The dispersion was influenced by the amount of added Mica, preferably using a higher than 1/1 Mica in weight. By visualization, Mica has an ability of subsiding the MEH-PPV aggregation in water. Under an ultraviolet light (Figure 1b), a color was illuminated, implying the enhancement of MEH-PPV dispersion in the presence of Mica. For comparison, the pristine MEH-PPV is in aggregated form, and the water solution showed no light emitting. In Figure 1c, the MEH-PPV dispersion by the assistance of different clays is demonstrated. Both MEH-PPV/Mica and MEH-PPV/MMT solutions demonstrated a deep-red appearance, while MEH-PPV/SWN and MEH-PPV/LDH revealed a light-red color, indicating the clay efficiency. Similar results were obtained for other CPs such as SPA and TPOPA, as indicated in Figure 1d and e.

The dispersion is examined by UV−visible absorbance, shown in Figure 2a. The Mica is most effective for enhancing the MEH-PPV dispersion in comparison with other clays. On the basis of the same weight ratio (MEH-PPV/clay = 1/1), the intensity for MEH-PPV/Mica is higher than that using other clays. In considering the ionic charges, LDH possesses cationic charges on the platelet surface and nitrate anionic species as the counterions. The ionic charge interaction between MEH-

PPV and clay through the clay surface anions (≡SiO^-) in MMT and Mica structures or cations ($[Mg_6Al_2(OH)_{16}]^+$) in LDH may be another factor for affecting the MEH-PPV dispersion. According to the UV−vis absorbance in Figure 2b, the MEH-PPV dispersion is closely correlated to the amount of Mica addition. The absorbance at 524 nm becomes more intensive with the increasing amount of Mica, implying the improvement of MEH-PPV dispersion. The control experiment for the pristine Mica indicates that the increasing absorbance of UV−vis is fully contributed from MEH-PPV in water. For other CPs, the absorbance of SPA/Mica and TPOPA/Mica also increased by the Mica enhancement.

The dispersion of the CP/clay hybrid in water was further observed by TEM. In Figure 3a, c, and e, the micrograms with a low magnification of MEH-PPV/Mica, SPA/Mica, and TPOPA/Mica hybrids all revealed a homogeneous distribution. Under high magnification in Figure 3b, d, and f, shown are the morphology of Mica in a platelet-like shape with dimension of 300−1000 nm and the particle size of CPs at 1 μm for MEH-PPV, 10−100 nm for SPA, and 100 nm for TPOPA. These images were taken by dropping the dispersed solution on the copper grid of the TEM sample holder. The observed images can only be extrapolated to the solution dispersion state. The MEH-PPV conjugated polymer appeared to have larger aggregated particles than that of SPA and TPOPA. The particle size measurements from TEM are well correlated to the zetasizer analysis (Supporting Information, Table S1 and Figure S5). By comparison to MEH-PPV, the pristine Mica has an average particle size (APS) of 152 μm but decreased from 152 to 2 μm when hybridizing with MEH-PPV through the grinding procedure. It is noted that the size analysis is a relative correlation without considering the deviation from the platelet shape of the clay particle. The zeta potentials (Supporting Information, Table S2) for MEH-PPV in mixing with three clays were investigated. Negative zeta potentials remained when hybridizing with Mica or MMT, in contrast to the use of LDH. Due to the anionic LDH property, the MEH-PPV/LDH hybrid showed a zero zeta potential due to the opposite charge attraction and solution precipitation. It is interestingly noted that the zeta potential measurements could differentiate the MEH-PPV interaction with anionic LDH from cationic clays (Mica and MMT).

3.2. Optical Performance of CP/Mica Hybrids. The degree of dispersion influences the optical property of CPs. Photoluminescence spectrophotometry (PL) was performed at an excited wavelength of 524 nm that corresponded to the inherent MEH-PPV properties. The PL intensity is rated by the following trend: MEH-PPV/Mica > MEH-PPV/MMT > MEH-PPV/SWN > MEH-PPV/LDH, as indicated by Figure 4a. The trend of the PL emission reflected the degree of MEH-PPV dispersion in water, and the PL trend is consistent with the UV−vis absorbance. The Mica clay appears to perform better than other clays tested. The content of Mica has a slight influence on the PL spectrum of MEH-PPV/Mica due to the variation of dispersion (Figure 4b). The PL spectrum of MEH-PPV/Mica has a slightly blue shift from 601 to 595 nm corresponding to the amount of Mica present. The blue shift of MEH-PPV/Mica is due to the variation of CP conjugated length.[44]

The MEH-PPV/Mica films prepared from the corresponding solution precursor were shown to have UV−vis and PL properties (Figure 5). For the MEH-PPV/Mica (weight ratio = 1/1) film as shown in Figure 5a, there exist a maximal absorbance at $\lambda_{max.abs.}$ = 580 nm and a maximum emission at $\lambda_{max.em.}$ = 605 nm. In the inset, the film exhibited a noticeable orange light emission when exposed to a UV lamp. The orange

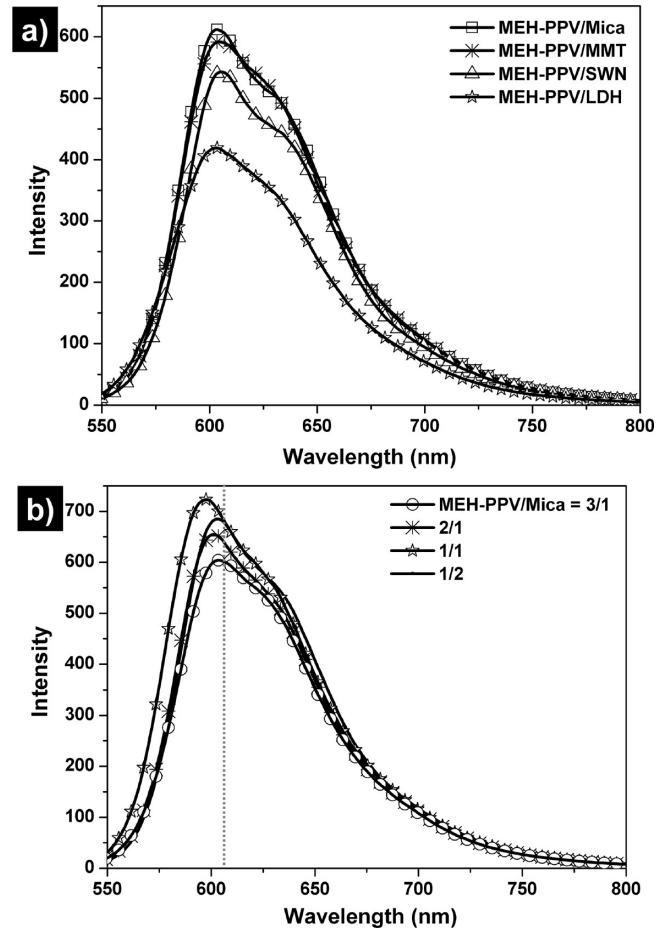

Figure 4. PL spectra of CP/clay solution (a) with different clay and (b) with Mica but different weight ratio.

light is exactly correlated to the PL at 605 nm. In Figure 5b, the SPA/Mica film has a spectrum at $\lambda_{max.abs.}$ = 425 nm and $\lambda_{max.em.}$ = 560 nm, with the corresponding olive light emitting under a UV lamp. For the TPOPA/Mica film, in Figure 5c, the results of $\lambda_{max.abs.}$ = 430 nm and $\lambda_{max.em.}$ = 530 nm were obtained. Green light emission corresponded to the PL of 530 nm.

3.3. Explanation for the Dispersion Behavior of CP/Clay. The dispersion of CPs into the water phase in the presence of the ionic clays is first rationalized by noncovalent bonding forces. The CPs are hydrophobic and only soluble in organic mediums. In water, the polymers are in aggregates or precipitates due to molecular−coil entanglement. Both UV−vis absorbance and TEM observation confirmed the fine distribution of the CP/Clay hybrids in aqueous dispersion. As illustrated by GSI conception in Figure 6, the initial grinding of two distinctly different materials in the nanometer scale may have homogenized two different materials in the micrometer scale. When dispersing into water, the strong noncovalent bonding force between clay and water molecules could further exclude the CP molecular self-aggregation. Both of the mutual interactions through noncovalent bonding forces such as ionic charges for the clay surface, van der Waals force and $\pi-\pi$ stacking for CP entanglement attraction, and the platelike geometric shape blockage could all together influence the CP pristine aggregation. In other words, the CP polymer entanglement is mitigated and physically blocked by the neighboring Mica platelets. The presence of clay colloid in water effectively rendered the CP dispersion in water. The overall effect is to disperse CPs without going through a tedious chemical modification. It also implies

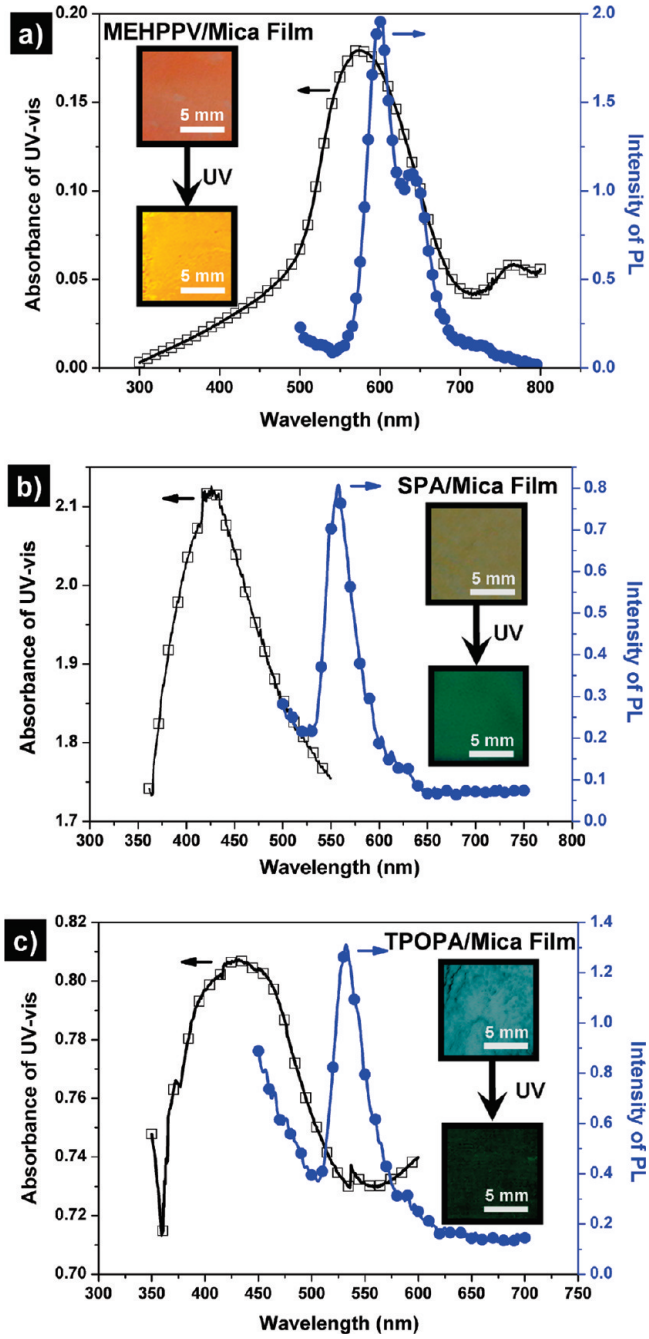

Figure 5. UV−vis and PL spectra of the hybrid film of MEH-PPV/Mica (a), SPA/Mica (b), and TPOPA/Mica (c).

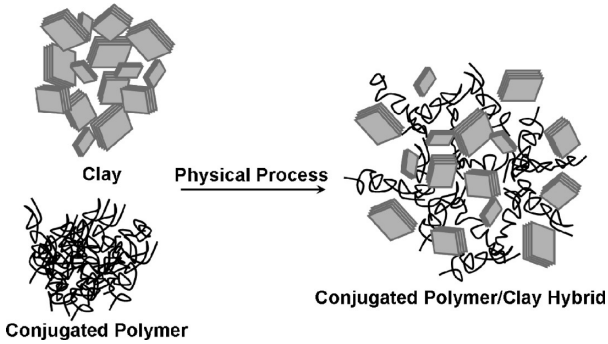

Figure 6. Conceptual illustration of homogeneous distribution between clay and CP through redistribution of noncovalent bonding forces of the CP coils and rigid clay units.

the "green process" is possibly generalized for other hydrophobic polymers.

4. Conclusion

By simply pulverizing CPs with Mica, the powder mixture became conveniently dispersible in water. The fluorinated Mica is the best dispersing agent among the screened clays including MMT, SWN, and LDH. The dispersion enhancement is measured by UV−vis absorbance in water. Three CPs (MEH-PPV, SPA, and TPOPA) were used to generalize this colloidal process for dispersing CPs. The CP films were prepared and demonstrated for their photoluminescence properties. There are observed maximum emissions at 605, 560, and 530 nm for three CPs and the corresponding color emission, orange, olive, and green, under a UV lamp. The dispersion mechanism is explained by noncovalent bonding redistribution in water medium and also by a geometric shape exclusion effect derived from the high aspect ratio plate structure. The dispersing CPs in the Mica colloid provide a solvent-free method for preparing CPs films and broaden the CP applications.

Acknowledgment. We acknowledge financial support from the Ministry of Economic Affairs and the National Science Council (NSC) of Taiwan.

Supporting Information Available: Chemical structures and SEM of the conjugated polymers (Figures S1−4), particle size (Figure S5 and Table S1), and zeta potential (Table S2) of Mica/MEH-PPV are provided. This material is available free of charge via the Internet at http://pubs.acs.org.

References and Notes

(1) Karakaya, B.; Claussen, W.; Gessler, K.; Saenger, W.; Schlüter, A. D. *J. Am. Chem. Soc.* **1997**, *119*, 3296–3301.
(2) Stocker, W.; Karakaya, B.; Schürmann, B. L.; Rabe, J. P.; Schlüter, A. D. *J. Am. Chem. Soc.* **1998**, *120*, 7691–7695.
(3) Bo, Z. S.; Rabe, J. P.; Schlüter, A. D. *Angew. Chem., Int. Ed.* **1999**, *38*, 2370–2372.
(4) Bao, Z. N.; Amundson, K. R.; Lovinger, A. J. *Macromolecules* **1998**, *31*, 8647–8649.
(5) Sato, T.; Jiang, D. L.; Aida, T. *J. Am. Chem. Soc.* **1999**, *121*, 10658–10659.
(6) MacDiarmid, A. G. *Synth. Met.* **1997**, *84*, 27–34.
(7) Lee, R. H.; Lai, H. S.; Wang, J. J.; Jeng, R. J.; Lin, J. J. *Thin Solid Films* **2008**, *517*, 500–505.
(8) Schenning, A. P. H. J.; Martin, R. E.; Ito, M.; Diederich, F.; Boudon, C.; Gisselbrecht, J. P.; Gross, M. *Chem. Commun.* **1998**, 1013–1014.
(9) Kaneko, T.; Horie, T.; Asano, M.; Aoki, T.; Oikawa, E. *Macromolecules* **1997**, *30*, 3118–3121.
(10) Sirringhaus, H.; Brown, P. J.; Friend, R. H.; Nielsen, M. M.; Bechgaard, K.; Langeveld-Voss, B. M. W.; Spiering, A. J. H.; Janssen, R. A. J.; Meijer, E. W.; Herwig, P.; de Leeuw, D. M. *Nature* **1999**, *401*, 685–688.
(11) Morin, J. F.; Leclerc, M.; Ades, D.; Siove, A. *Macromol. Rapid Commun.* **2005**, *26*, 761–778.
(12) Müllen, K.; Meghdadi, F.; List, E. J. W.; Leising, G. *J. Am. Chem. Soc.* **2001**, *123*, 946–953.
(13) Chou, C. H.; Shu, C. F. *Macromolecules* **2002**, *35*, 9673–9677.
(14) Lee, D. W.; Swager, T. M. *Synlett* **2004**, 149–154.
(15) Korri-Youssoufi, H.; Yassar, A. *Biomacromolecules* **2001**, *2*, 58–64.
(16) Satrijo, A.; Swager, T. M. *J. Am. Chem. Soc.* **2007**, *129*, 16020–16028.
(17) Kumaraswamy, S.; Bergstedt, T.; Shi, X.; Rininsland, F.; Kushon, S.; Xia, W. S.; Ley, K.; Achyuthan, K.; McBranch, D.; Whitten, D. G. *Proc. Natl. Acad. Sci. U.S.A.* **2004**, *101*, 7511–7515.
(18) Pinto, M. R.; Schanze, K. S. *Proc. Natl. Acad. Sci. U.S.A.* **2004**, *101*, 7505–7510.
(19) McGehee, M. D.; Heeger, A. J. *Adv. Mater.* **2000**, *12*, 1655–1668.
(20) McQuade, D. T.; Pullen, A. E.; Swager, T. M. *Chem. Rev.* **2000**, *100*, 2537–2574.
(21) Faid, K.; Leclerc, M. *Chem. Commun.* **1996**, 2761–2762.

(22) Yang, C. Y.; Mauricio, P. J.; Schanze, K.; Tan, W. H. *Angew. Chem., Int. Ed.* **2005**, *44*, 2572–2576.
(23) Islam, M. F.; Rojas, E.; Bergey, D.; Johnson, M.; A. T.; Yodh, A. G. *Nano Lett.* **2003**, *3*, 269–273.
(24) Lee, K. W.; Povlich, L. K.; Kim, J. *Adv. Funct. Mater.* **2007**, *17*, 2580–2587.
(25) Patil, A. O.; Ikenoue, Y.; Wudl, F.; Heeger, A. J. *J. Am. Chem. Soc.* **1987**, *109*, 1858–1859.
(26) Pickup, P. *J. Electroanal. Chem.* **1987**, *225*, 273–280.
(27) Shi, S.; Wudl, F. *Macromolecules* **1990**, *23*, 2119–2124.
(28) Wallow, T. I.; Novak, B. M. *J. Am. Chem. Soc.* **1991**, *113*, 7411–7412.
(29) Child, A. D.; Reynolds, J. R. *Macromolecules* **1994**, *27*, 1975–1977.
(30) Balanda, P. B.; Ramey, M. B.; Reynolds, J. R. *Macromolecules* **1999**, *32*, 3970–3978.
(31) Pai, Y. H.; Ke, J. H.; Chouc, C. C.; Lin, J. J.; Zen, J. M.; Shieu, F. S. *J. Power Sources* **2006**, *163*, 398–402.
(32) Dong, R. X.; Chouc, C. C.; Lin, J. J. *J. Mater. Chem.* **2009**, *19*, 2184–2188.
(33) Lan, Y. F.; Lin, J. J. *J. Phys. Chem. A* **2009**, *113*, 8654–8659.
(34) Lee, R. H.; Hsiue, G. H.; Jeng, R. J. *Polymer* **1998**, *40*, 13–19.
(35) Pinnavaia, T. J. *Science* **1983**, *220*, 365–371.
(36) Qi, G.; Yang, Y.; Yan, H.; Guan, L.; Li, Y.; Qiu, X.; Wang, C. *J. Phys. Chem. C* **2009**, *113*, 204–207.
(37) Saito, T.; Okamoto, M.; Hiroi, R.; Yamamoto, M.; Shiroi, T. *Macromol. Mater. Eng.* **2006**, *291*, 1367–1374.
(38) Utracki, L. A.; Sepehr, M.; Boccaleri, E. *Polym. Adv. Technol.* **2007**, *18*, 1–37.
(39) Lin, J. J.; Chen, Y. M. *Langmuir* **2004**, *20*, 4261–4264.
(40) Chan, Y. N.; Juang, T. Y.; Liao, Y. L.; Dai, S. A.; Lin, J. J. *Polymer* **2008**, *49*, 4796–4801.
(41) Rives, V.; Ulibarri, M. A. *Coord. Chem. Rev.* **1999**, *181*, 61–120.
(42) Rives, V. *Mater. Chem. Phys.* **2002**, *75*, 19–25.
(43) Roto, R.; Villemure, G. *J. Electroanal. Chem.* **2006**, *588*, 140–146.
(44) Traiphol, R.; Sanguansat, P.; Srikhirin, T.; Kerdcharoen, T.; Osotchan, T. *Macromolecules* **2006**, *39*, 1165–1172.

JP911117M